ANTIOXIDANTS & REDOX SIGNALING
Volume 9, Number 11, 2007

DOI: 10.1089/ars.2007.1921

Forum Original Research Communication

Promoter Elements Responsible for Antioxidant Regulation of MCP-1 Gene Expression

LIYU XING and DANIEL G. REMICK

ABSTRACT

Monocyte chemoattractant protein-1 (MCP-1) is produced by different cells in response to inflammatory stimulation. In the present study, a series of human MCP-1 promoter reporter genes were constructed to illustrate elements involved in antioxidant dimethyl sulfoxide (DMSO) inhibition of MCP-1 gene expression. MCP-1 secretion and mRNA expression and transcription activity stimulated by TNF-α or IL-1β were significantly inhibited by 1% DMSO in alveolar type II epithelial cells (A549). Deletion of −7537 to −2741 caused a 77% decrease in reporter activity, but DMSO inhibition was still present. Deletion of −7537 to −2616 containing the A1 NF-κB binding site resulted in a complete loss of MCP-1 stimulation. Deletion of −2585 to −74 decreased reporter activity by ∼50%, and DMSO inhibited this induction. Deletion of −2614 to −74 containing the A2 NF-κB binding site completely abolished responses to stimulation. Mutations of either of the NF-κB binding sites decreased promoter activity, which could still be inhibited by DMSO, whereas deletion of both NF-κB binding sites abolished induced transcriptional activity. Mutation or deletion of the NF-κB binding sites significantly decreased or abolished reporter activity in response to reactive oxygen intermediates (ROI), generated by xanthine plus xanthine oxidase. In conclusion, DMSO inhibits MCP-1 gene expression through both NF-κB binding sites located far upstream of the 5′-flanking region of the MCP-1 promoter. *Antioxid. Redox Signal.* 9, 1979—1989.

INTRODUCTION

Blood monocytes infiltrate into the sites of inflammation and play major roles in host defense through their ability to present antigens and to produce various mediators. Although the mechanisms of monocyte infiltration have not been fully understood, locally produced monocyte chemoattractants appear to be responsible for the recruitment of blood monocytes into the sites of inflammatory reactions.

Monocyte chemoattractant protein-1 (MCP-1) is a member of the CC subfamily of the chemokines and attracts blood monocytes both *in vitro* and *in vivo* (1). MCP-1 was initially characterized as a monocyte-specific chemoattractant *in vitro* (34), but was subsequently shown also to attract memory T lymphocytes, natural killer cells, and neutrophils. A wide variety of cells, including monocytes, fibroblasts, vascular endothelial cells, and smooth muscle cells, produce MCP-1 *in vitro* in response to stimuli such as IL-1, TNF-α, platelet-derived growth factor, IFN-γ, and lipopolysaccharide (LPS). MCP-1 has been implicated in the pathology of various diseases characterized by a mononuclear cell infiltrate. Rosseau *et al.* (26) reported that upregulation of MCP-1 synthesis and its secretion into the alveolar space is the central event in the early expansion of the alveolar mononuclear phagocyte population observed in patients with ARDS, mainly because of a rapid influx of monocytes from the vascular compartment. These events were found to be significantly correlated with the severity of respiratory failure.

Reactive oxygen intermediates (ROIs) are widely involved in different phases of the inflammatory reaction. Recent studies have linked oxidants to stimulation of cytokine and chemokine production through modulation of certain transcriptional

[1]Department of Pathology University of Michigan, Medical School, Ann Arbor, Michigan.

activating proteins (17, 19, 27). Other studies (30, 32) showed that ROIs, such as those generated by hyperoxia, have an effect on MCP-1 and IL-8 production (6). ROIs have also been shown to be necessary intermediates in calcium oxalate crystal–induced MCP-1 production (33). MCP-1 production is enhanced by a variety of oxidants through increased transcription (32). Previous work demonstrated that treatment with the antioxidant DMSO attenuates LPS-induced secretion of the CXC chemokine IL-8 (8, 30), supporting the hypothesis that oxidants may act as second messengers in the initiation of chemokine gene activation. DMSO does not globally suppress all gene activation; we previously reported that DMSO will actually augment IL-1β production (36).

To understand the mechanism(s) of ROI regulation of human MCP-1 gene expression, we investigated DMSO modulation of TNF-α–induced and IL-1β–induced MCP-1 secretion, mRNA expression, and transcriptional activity. TNF-α and IL-1β have been used as classic stimuli to induce cell activation (35). Human type II alveolar epithelial cells, A549 cells, were used for these studies. Special attention was paid to identifying specific promoter elements responding to DMSO in MCP-1 gene expression at the transcriptional level by using the whole 5′-flanking region of the human MCP-1 gene.

MATERIALS AND METHODS

Reagents and materials

A549 cells were purchased from American Type Culture Collection (Manassas, VA). The polyriboprobe set hCK-5, the *in vitro* transcription kit, and the RPA kit were obtained from Pharmingen (San Diego, CA). [α-^{32}P]UTP was purchased from New England Nuclear (Cambridge, MA). The Lipofectamine+Plus reagent transfection kit and Zero Blunt TOPO PCR Cloning Kit were from Invitrogen (Carlsbad, CA). EDTA, DMSO, DMTU, and TMB were obtained from Sigma (St. Louis, MO). The human TNF-α, IL-6, MCP-1, and IL-1β standards, as well as the capture and biotin-conjugated detection antibodies for the IL-6 and MCP-1 ELISAs were purchased from R&D (Minneapolis, MN). Horseradish peroxidase–conjugated streptavidin was purchased from Jackson ImmunoResearch Laboratories, Inc. (West Grove, PA). The blocking solutions, Blotto and Casein, were obtained from Pierce (Rockford, IL). Glutamine, heat-inactivated fetal bovine serum (FBS), trypsin (0.125%), and Dulbecco's phosphate-buffered saline were obtained from Gibco BRL (Grand Island, NY). Dulbecco's modified Eagle's medium (DMEM), penicillin, and streptomycin were obtained from Bio-Whittaker (Walkersville, MD). Erase-A-Base kit, Exonuclease III, S1 nuclease, Klenow DNA polymerase, the pGL-3 basic vector, the pRL-TK vector, the Dual-Luciferase Reporter Assay System, the Wizard Genomic DNA Purification Kit, Wizard Plus SV Miniprep DNA purification system, and restriction enzymes were from Promega (Madison, WI). The EndoFree Plasmid Maxi Kit was from Qiagen (Valencia, CA). The Expand High Fidelity PCR System was from Roche (Indianapolis, IN). The LightShift EMSA kit, NE-PER Nuclear and Cytoplasmic Extraction Reagents and Halt Protease Inhibitor Cocktail kit were from Pierce (Rockford, IL). NF-κB consensus oligonucleotides were synthesized with a biotin label on the 5′ end by Sigma Genosis (Woodlands, TX). The sequence is 5′-AGT TGA GGG GAC TTT CCC AGG C-3′.

Cell culture

The A549 cells were grown as a monolayer in tissue-culture flasks (Nunc, Naperville, IL) in 100% humidity and 5% CO_2 at 37°C. DMEM with 10% FCS, penicillin (50 U/ml), streptomycin (50 μg/ml), and HEPES (25 m*M*) was used for culture media. The cells were harvested with trypsin (0.125%). For each experiment, the A549 cells were plated in 24-well culture plates at a density of 1×10^5 cells/well and were grown for 36 h to confluence in DMEM with 10% FCS. Confluent cells were washed free of FCS with Dulbecco's phosphate-buffered saline and cultured in FCS-free DMEM for 48 h. On the day of use, the A549 cell monolayer was washed with Dulbecco's phosphate-buffered saline. The cells were preincubated with DMSO immediately before TNF-α or IL-1β stimulation in FCS-free DMEM.

Enzyme-linked immunosorbent assay (ELISA)

Culture supernatants from stimulated A549 cells were removed, and MCP-1 and IL-6 concentrations were measured with ELISAs, according to our previously published methods (3, 20). Cytokine concentrations were calculated based on standard curves.

RNA preparation

Clean instruments were used for each cell sample to eliminate cross contamination. Total RNA was extracted by using the acid guanidinium thiocyanate-phenol-chloroform extraction procedure (7). In brief, the cells were homogenized in guanidinium thiocyanate followed by acid phenol/chloroform extraction and precipitated with isopropanol.

Ribonuclease protection assay (RPA)

The RPA was performed by following the instructions from Pharmingen. Riboprobe syntheses were driven by the T7 bacteriophage RNA polymerase with [α-^{32}P]UTP as the labeling nucleotide. The ^{32}P-probe (6×10^5 cpm/sample) was added to tubes containing the sample RNA (4 μg) dissolved in 8 μl hybridization buffer. The samples were heated to 90°C, the temperature decreased, and RNase T1 added, followed by treatment with proteinase K. The RNA duplexes were isolated by extraction/precipitation as described earlier, dissolved in 5 μl gel-loading buffer, and electrophoresed in standard 5% acrylamide/8 *M* urea sequencing gels. The gel was dried and placed on XAR film (Eastman Kodak Company, Rochester, NY) with intensifying screens and was developed at −70°C for 4–12 h.

Construction of reporter vectors

The pGL-3 basic vector was used to construct the pGL-3 basic-human MCP-1 promoter region reporter vector (pGL-3-

MCP-1). The sequence of the human MCP-1 gene (Y18933) was obtained from the National Center for Biotechnology Information (11). Primers used to construct the reporter vectors are listed in Table 1. The promoter region of human MCP-1 was amplified by using the Expand High Fidelity PCR System with chemically synthesized primers and genomic DNA as a template. The PCR fragment was cloned into the Zero Blunt TOPO PCR Cloning vector. The insert positive vector was digested with Acc 65I and Mlu I, and then the MCP-1 promoter fragment was subcloned into the Acc 65I (Kpn I)-Mlu I site of the pGL-3 basic vector to generate the reporter vector.

Generation of 5′ or 3′ deletions of MCP-1 promoter region

To generate a series of 5′ end deletions, the reporter vector was digested with Kpn I and Bst 981 to generate 3′ and 5′ overhangs. The digested vector was subjected to Exonuclease III to generate a series of 5′ end deletions. Aliquots of the reaction mixture were removed at specific time points and digested with S1 nuclease, and the size of the deleted vectors was determined by electrophoresis. After the ends were incubated with Klenow DNA polymerase, the vectors were religated. These "deleted" vectors were also sequenced to verify the 5′ end of MCP-1 promoter region (shown schematically in Results).

According to the locations of the two NF-κB binding sites (A1 and A2 sites), the GC box and TATA box reported by Ueda *et al.* (31, 32), a series of 3′ deletions were generated by two PCR reactions. Fragment −72 to +8, containing the GC box and the TATA box, which maintains the basal transcriptional activity of the MCP-1 gene, was obtained with primer pair 3+4 (see Table 1 for the primers) and cloned into the NheI–Bgl II of pGL-3 basic vector. Fragments −7537 to −6489, −7537 to −2647, −7537 to −2614, and −7537 to −2586 were amplified by PCR and cloned into the Zero Blunt TOPO PCR Cloning vector. The cloning vectors were digested with Acc 65I (Kpn1) and Mlu I. The target fragments were cloned into the Acc 65I (Kpn I)-Mlu I site of the pGL-3 basic vector upstream of the MCP-1 GC box and TATA box fragments. In this way, four vectors were made in which fragments bp −6488 to −74, bp −2648 to −74 containing both A1 and A2 NF-κB binding sites, −2615 to −74 containing A2 NF-κB binding site, and −2587 to −74 were deleted, respectively (shown schematically in Results).

PCR mutagenesis

Site-directed mutagenesis of both NF-κB binding sites was performed by two PCR reactions with two pairs of primers (Table 1) and genomic DNA as the template. Two overlapping primers, sense and antisense, were designed for the mutation sites. The overlapping portions were the mutation sites in which the corresponding bases were replaced to generate a MluI restriction site at the 5′ end of the primers. These two PCR fragments were cloned into the vector. MluI and XmaI digested the cloning vector containing the downstream fragment of the MCP-1 promoter region. The target fragments were ligated into the MluI–XmaI site of the pGL-3 basic vector. The cloning vector, containing the upstream fragment of the MCP-1 promoter region, was digested by KpnI + MluI. The target fragment was ligated into the KpnI–MluI site of the pGL-3 basic vector containing the downstream fragment. All mutations were verified by DNA sequencing (shown schematically in Fig. 8).

Transfection and luciferase assays

Transient co-transfection with the pGL-3 reporter vector and the control vector pRL-TK vector into A549 cells was performed by using the Lipofectamine+Plus method. The total amount of DNA was 0.4 μg/well. The molar ratio of the pGL-3 reporter vector to the pRL-TK control vector was 10:1. Because of the different lengths of inserts, the difference in the amount of DNA was supplemented with the pGL-3 basic vector. The construction and transfection of the DNA complex were performed by following the manufacturer's protocol. After incubation of A549 cells with DNA for 6 h, DMEM with serum was added to achieve a final serum concentration of 10%. Meanwhile, human TNF-α (2 ng/ml) or human IL-1β (1 ng/ml)

TABLE 1. DEOXYOLIGONUCLEOTIDES USED FOR PCR AND SEQUENCING ANALYSIS

No.	*Sequence*	*Site*	*Primer*	*Restriction site*
1	5′-AGCCTTGGCCACAGTGTCATCC-3′	−7537 to −7515	Sense	
2	3′-CCTTGGCTCTCCGACTCTGCGCA-5′	−11 to +11	Anti-sense	MluI
3	5′-GCTAGCCTCCGCCCTCTCTCCC-3′	−73 to −53	Sense	NheI
4	3′-CCTTGGCTCTCCGACTCTAGA-5′	−10 to +8	Anti-sense	BglII
5	3′-GTCGAAGGAAGGAGTCTGCGCA-5′	−6511 to −6489	Anti-sense	MluI
6	3′-GGTTTACGTAAGAGAAGATGCGCA-5′	−2671 to −2647	Anti-sense	MluI
7	3′-GTTTCGACGGAGGAGTGCGCA-5′	−2636 to −2614	Anti-sense	MluI
8	3′-GGTGAGTGAAGAGAGTGCGCA-5′	−2607 to −2586	Anti-sense	MluI
9	3′-GCTCTCCGACTCTGATTGGGCCC-5′	−7 to +16	Anti-sense	XmaI
10	3′-GTAAGAGAAGATGCCCTAGACTGCGCA-5′	−2665 to −2638	Anti-sense	MluI
11	5′-ACGCGTTCCAAAGCTGCCTCCTCA-3′	−2644 to −2619	Sense	MluI
12	3′-GTTTCGACGGAGGAGTCTCACTGCGCA-5′	−2636 to −2619	Anti-sense	MluI
13	5′-ACGCGTTGCACTCACTTCTCTCAC-3′	−2615 to −2590	Sense	MluI
14	5′-CTAGCAAAATAGGCTGTCCC-3′	Sequencing	Sense	
15	5′-CTTTATGTTTTTGGCGTCTTCAC-3′	Sequencing	Anti-sense	

was added to the medium to stimulate the cells for 6 h. The cells were washed with PBS without Ca^{2+} and Mg^{2+} twice, and then 100 μl 5X passive lysis buffer/well was added. The plate was shaken for 15 min at room temperature, and then stored at −70 °C.

After preparation of the cell extract, luciferase activities were measured by using the Dual-Luciferase Reporter Assay System and Packard LumiCount BL10000 (Packard Instrument Co., Boston, MA). The activities of the reporter vectors were reported as the ratio of firefly luciferase to the Renilla control vector. The basal activity level was subtracted. The percentage of activity inhibition by DMSO was expressed as (stimulus - stimulus plus DMSO)/stimulus.

The percentage suppression by DMSO was calculated for the different reporter constructs with the equation indicated in the figure. This was performed to demonstrate the relative reduction in reporter activity.

Electrophoretic mobility shift assay (EMSA)

A549 cells were cultured in serum-free medium for 48 h, stimulated with TNF-α (2.0 ng/ml) or IL-1β (1.0 ng/ml) for 30 min, and washed in ice-cold PBS. Nuclear extracts were prepared by using the NE-PER Nuclear and Cytoplasmic Extraction Reagents by following the manufacturer's instructions. The protein concentration was determined with a Bradford Assay.

Binding reactions were performed by using LightShift EMSA kit according to the manufacturer's instructions: 20 fmol biotin end-labeled NF-κB consensus oligonucleotides and 5 μg of nuclear extract were present in 20 μl reaction volume. Reactions were incubated for 15 min at room temperature, and DNA–protein complexes were analyzed by electrophoresis on a 6% native polyacrylamide gel in 0.5X TBE buffer at 4°C.

Statistics

Results were reported as mean ± SEM. Statistical comparisons were performed by using a one-way ANOVA with the Tukey comparison test and *t* test. All analyses were performed by using GraphPad Prism (San Diego, CA).

RESULTS

DMSO inhibition of TNF-α– or IL-1β–induced MCP-1 production

Among the proinflammatory cytokines, TNF-α and IL-1β are important for the development of local inflammation and tissue damage, and these were selected for stimulating A549 cells. We examined the concentration range of TNF-α and IL-1β capable of inducing MCP-1 by incubating cells with increasing concentrations of TNF-α or IL-1β for 24 h. Both TNF-α and IL-1β significantly increased MCP-1 production by A549 cells in a dose-dependent manner (Fig. 1A and B). The MCP-1 levels in the culture supernatants continued to increase, even at the highest concentrations of TNF-α and IL-1β. IL-1β was a more potent stimulus for MCP-1 production compared with TNF-α.

To investigate whether ROIs mediate TNF-α– and IL-1β–induced MCP-1 synthesis by A549 cells, the cells were incubated with DMSO (1% vol/vol) immediately before TNF-α or IL-1β stimulation. As shown in Fig. 1A and B, DMSO significantly inhibited MCP-1 production induced by all concentrations of TNF-α or IL-1β.

Kinetic experiments showed that both 1,000 pg/ml TNF-α and 300 pg/ml IL-1β stimulated MCP-1 production by A549 cell in a time-dependent manner. As shown in Fig. 2A and B, both cytokines markedly increased MCP-1 secretion over that spontaneously released from nonstimulated cells. The kinetics of TNF-α and IL-1β induction of MCP-1 was similar, although IL-1β once again showed more potent induction. Both IL-1β and TNF-α induced MCP-1 secretion that was detectable as early as 2 h, and MCP-1 continued to increase up to 24 h. Pretreatment of the cells with DMSO inhibited TNF-α– or IL-1β–induced MCP-1 secretion from 4 h up to 24 h after stimulation (Fig. 2A and B). Consistent with the data from the dose–response experiment, DMSO inhibited TNF-α– and IL-1β-induced MCP-1 secretion.

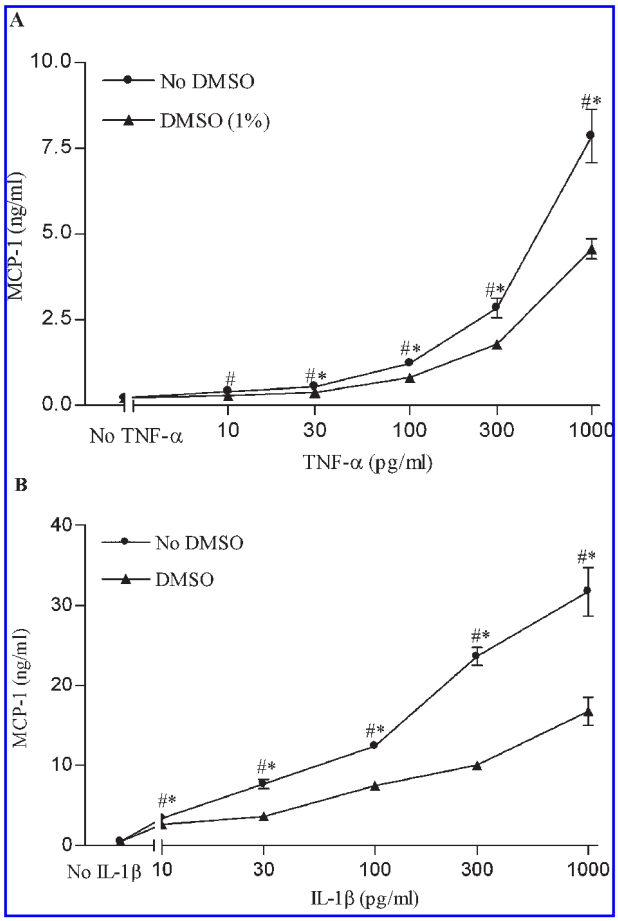

FIG. 1. DMSO inhibits dose-dependent TNF-α and IL-1β induced MCP-1. A549 cells were stimulated with increasing concentrations of human TNF-α (**A**) or IL-1β (**B**) (10–1,000 pg/ml) in the presence or absence of DMSO (1.0%) for 24 h. Data shown are the means ± SEM of four independent experiments. $^{\#}p < 0.05$ compared with no IL-1β or TNF-α; $^{*}p < 0.05$ compared with DMSO-treated cells. In some samples, the error bar is smaller than the symbol.

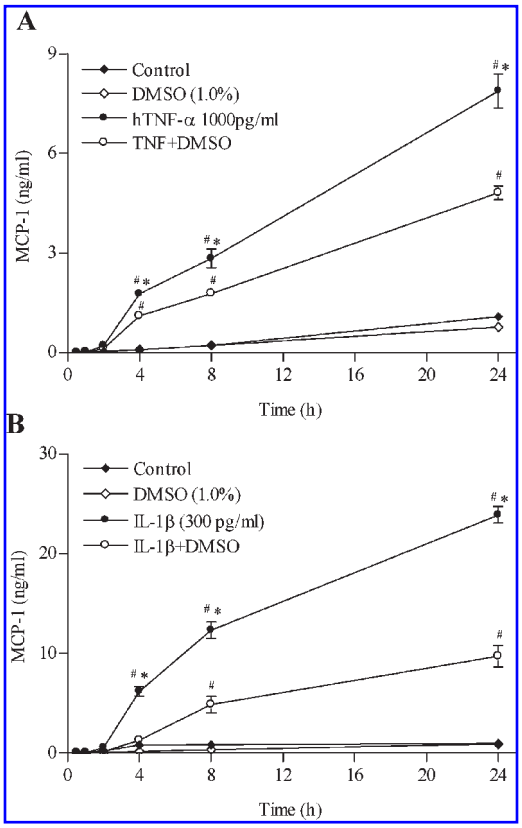

FIG. 2. DMSO inhibits TNF-α and IL-1β induction of MCP-1 at virtually all time points. A549 cells were stimulated with human TNF-α, 1,000 pg/ml (**A**), or IL-1β, 300 pg/ml (**B**), in the presence or absence of DMSO (1.0%) for 0.5–24 h. Data shown are means ± SEM of four independent experiments. $^{\#}p < 0.05$ compared with no IL-1β or TNF-α; $^{*}p < 0.05$ compared with DMSO-treated cells. In some samples, the error bar is smaller than the symbol.

Effect of DMSO on TNF-α– or IL-1β–stimulated expression of MCP-1 mRNA

To determine whether DMSO inhibited the MCP-1 mRNA level, MCP-1 mRNAs were measured with a ribonuclease protection assay (RPA). An additional advantage of the RPA is that we may determine whether TNF-α or IL-1β induces other chemokine mRNA in the A549 cell line.

Stimulation with TNF-α or IL-1β (10–1000 pg/ml) for 2 h increased MCP-1 mRNA expression in a dose-dependent manner (Fig. 3). DMSO (1%, vol/vol) decreased MCP-1 mRNA in A549 cells at each TNF-α and IL-1β dose. In parallel with the results from the secreted protein experiments, DMSO inhibited the TNF-α– and IL-1β–induced expression of MCP-1 mRNA.

With the poly-riboprobe set, we detected both IL-8 mRNA and MCP-1 mRNA expression, but we did not detect mRNA expression for other chemokines after TNF-α or IL-1β stimulation of A549 cells (Ltn, RANTES, IP-10, MIP-1α, MIP-1β, or I-309). Consistent with a previous report (8), DMSO inhibited TNF-α– and IL-1β–induced IL-8 mRNA expression. Cell viability was not affected, as judged by the supernatant levels of TNF-α–stimulated IL-6 production, which were not suppressed.

DMTU also inhibits MCP-1 production

As an antioxidant, DMSO inhibited TNF-α– and IL-1β–induced MCP-1 gene expression. To provide further evidence that other antioxidants exhibit this same capacity to decrease MCP-1 production, DMTU was used to treat the A549 cells. As shown in Fig. 4, DMTU inhibited TNF-α (A)– and IL-1β (B)–induced MCP-1 production by A549 cells at concentrations of 10 m*M* and 20 m*M* without altering the cellular viability (data not

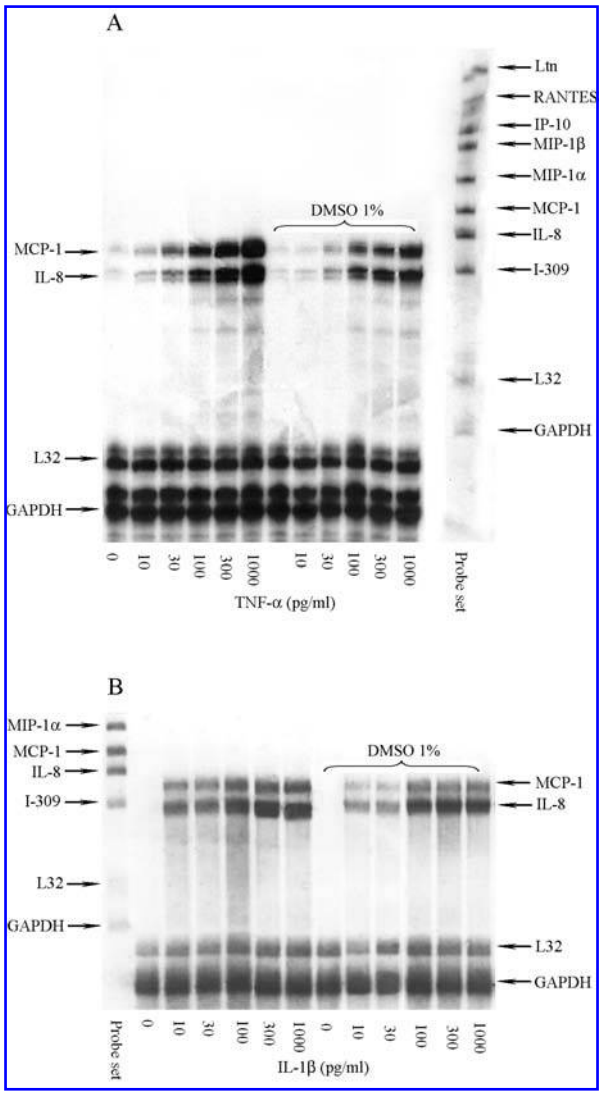

FIG. 3. DMSO inhibits MCP-1 at the level of mRNA. A549 cells were stimulated with human TNF-α or IL-1β in the presence or absence of 1% DMSO for 2 h. Total RNA was extracted and measured by the ribonuclease protection assay (RPA) for chemokine expression. The RPA demonstrates that TNF-α (**A**) or IL-1β induced (**B**) mRNA expression of MCP-1 in a dose-dependent manner in A549 cells. DMSO suppressed the cytokine-induced MCP-1 mRNA.

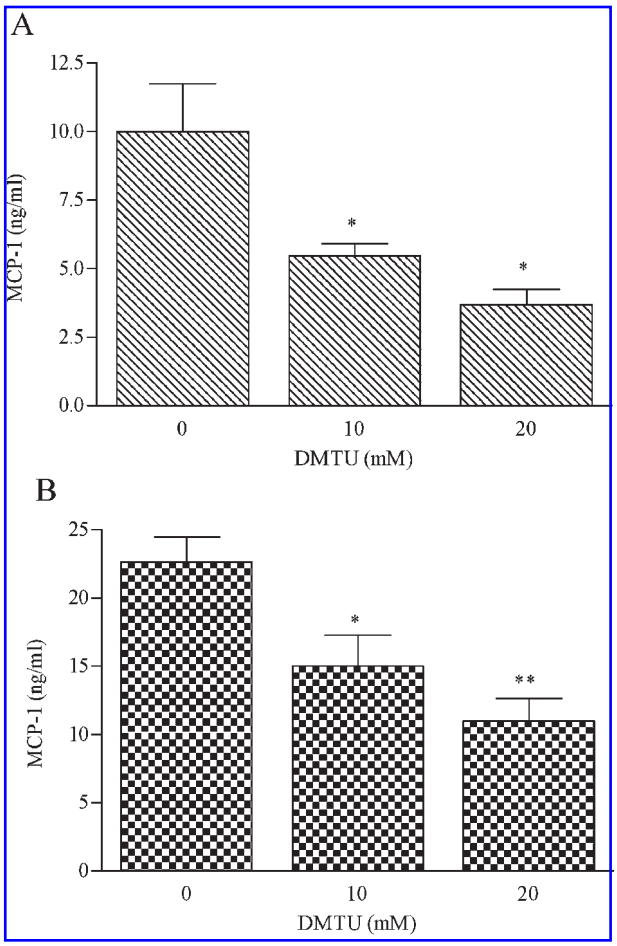

FIG. 4. Inhibition of cytokine-induced MCP-1 secretion by DMTU. A549 cells were simulated with human TNF-α (1,000 pg/ml) (**A**) or IL-1β (300 pg/ml) (**B**) in the presence of DMTU (0, 10, or 20 m*M*) for 24 h. Data shown are means ± SEM of four independent experiments. *$p < 0.05$; **$p < 0.01$ compared with no-DMTU treatment.

shown). These data indicate that the inhibitory effects of DMSO are due to the antioxidant capacity and not to nonspecific effects.

Inhibition of NF-κB by DMSO

NF-κB is involved in transcriptional regulation of a wide range of mediators, and a clear relation exists between ROIs and the nuclear transcription factor NF-κB (12, 18). We used the EMSA to determine whether DMSO inhibited the activation of NF-κB in response to TNF-α or IL-1β. As shown in Fig. 5, DMSO clearly suppressed the proinflammatory cytokine–induced activation of NF-κB in A549 cells. The two NF-κB binding sites, A1 and A2 are located far upstream of the 5′ promoter region of the MCP-1 gene (31). To confirm that DMSO inhibited MCP-1 gene expression at the level of transcription through these two NF-κB binding sites, and to ascertain whether other promoter elements were responsible for the inhibition by DMSO, a series of experiments was planned to map precisely those MCP-1 promoter elements that respond to antioxidant regulation.

Effect of 5′ deletion of MCP-1 promoter region on reporter activity

A549 cells were transiently transfected with either the pGL-3-MCP-1 vector or a series of pGL-3 vectors containing progressive 5′-deletions of the MCP-1 promoter. The pRL-TK vector was used as control of transfection efficiency. The constructs used are illustrated in Fig. 6A, and the results shown in Fig. 6B and C.

After transfection, A549 cells were stimulated with 2 ng/ml of TNF-α or 1 ng/ml of IL-1β for 6 h. As shown in Fig. 6B and C, the TNF-α– and IL-1β–induced activity of the full-length pGL-3-MCP-1 reporter vector was 303 ± 26 and 268 ± 33, respectively. DMSO inhibited TNF-α– and IL-1β–induced activity by 56% and 44%, respectively, supporting the hypothesis that DMSO suppressed TNF-α– and IL-1β–stimulated MCP-1 gene expression at the transcriptional level. The percentage of activity inhibition by DMSO was 59% and 44% in TNF-α– and IL-1β–stimulated A549 cells, respectively.

To determine whether DMSO inhibited MCP-1 gene expression through specific elements in the 5′-flanking region, A549 cells were transfected with a series of pGL-3 vectors containing progressive 5′-deletions of the MCP-1 promoter (described earlier). As shown in Fig. 6B and C, the inhibition of reporter activity by DMSO did not change significantly before

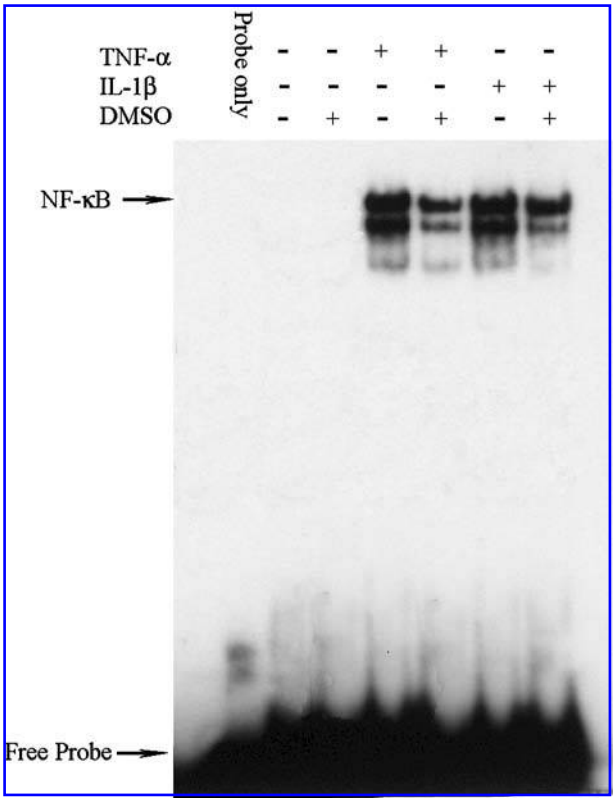

FIG. 5. DMSO inhibits NF-κB activation in A549 cells. The cells were incubated with 1% DMSO immediately before TNF-α (2 ng/ml) or IL-1β (1 ng/ml) stimulation (indicated by the top lines). After 30 min, the cells were harvested, and nuclear extracts were prepared. The EMSA gel is representative of three independent experiments.

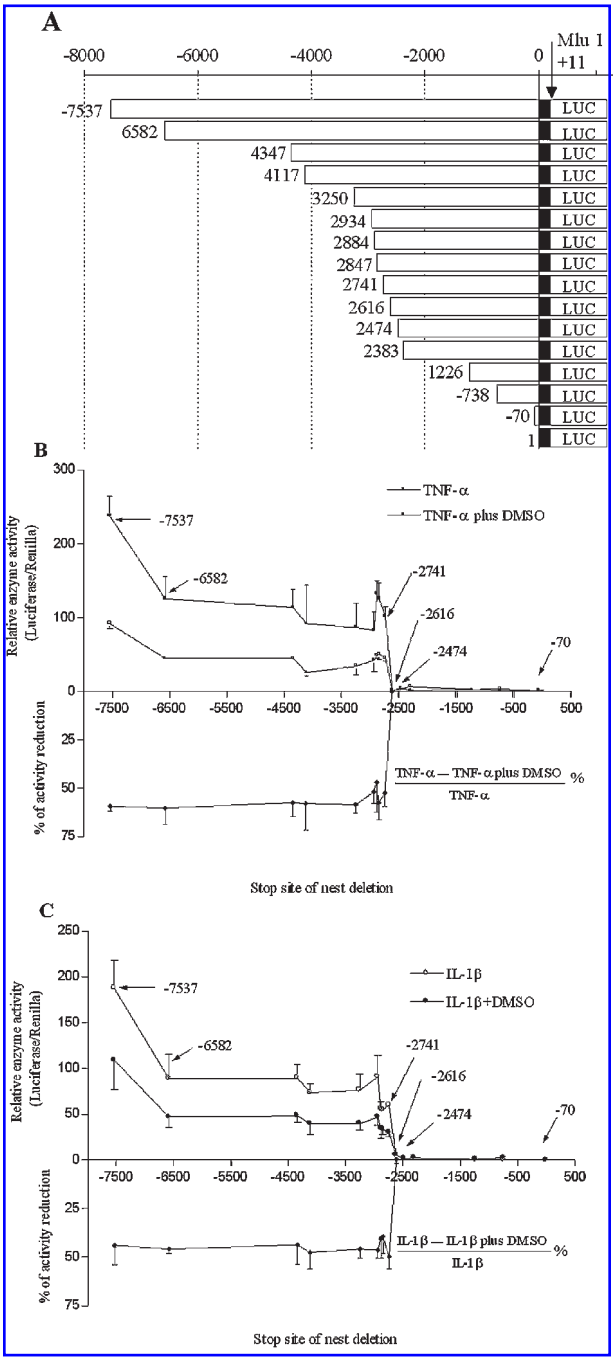

FIG. 6. Analysis of the human MCP-1 5′ flanking region. (**A**) The size of the 5′ promoter region of the MCP-1 linked to the luciferase gene fragment is indicated by the *open box* preceding the luciferase gene (LUC). The activity of each reporter vector is expressed as the ratio of firefly luciferase activity to *Renilla* luciferase activity in each cell extract after subtraction of the basal activity (**B, C**). The lower portion of each graph displays the percentage inhibition exerted by DMSO. The cells were stimulated with TNF-α (2 ng/ml; **B**) or IL-1β (1 ng/ml; **C**) in the presence or absence of DMSO. A dramatic loss of stimulated reporter activity occurs when the fragment length is decreased from −2741 to −2616. Each of the truncated reporters has nearly equivalent inhibition of activity by DMSO up to the point at which activity is no longer induced. The experiments were repeated four to 17 times, and the results are expressed as the mean ± SEM.

the small fragment −2741 to −2616 bp was further deleted, even though 5′-deletions of the MCP-1 promoter region between bp −7537 and −6582 resulted in a 36% and 45% decrease of induced reporter activity by TNF-α and IL-1β. With a further 5′-deletion of the small fragment (-2741 to −2616 bp), where the A1 NF-κB binding site is located, TNF-α and IL-1β could no longer induce MCP-1 reporter activity. Further deletions over −2616 toward downstream did not further alter the induction of TNF-α or IL-1β and the inhibition of DMSO on the activity of the MCP-1 reporter, as anticipated. To demonstrate that the induction of promoter activity up to site −2741 could always be suppressed by DMSO, the percentage reduction in activity is also displayed in the lower part of Fig. 6B and C. The data suggest that the elements located upstream of the A1 κB site are not involved in the inhibition of DMSO, although they participate in sustaining the maximal expression of the MCP-1 gene in response to proinflammatory cytokines.

Effect of 3′ deletions of MCP-1 promoter region on reporter activity

Figure 6 evaluated the effect of 5′ deletions on antioxidant regulation of MCP-1. To clarify the relation between the NF-κB binding sites and other potential transcription factor binding sites, and whether DMSO modulates transcription factor binding at these sites, a series of pGL-3 vectors containing 3′ deletions of the promoter region of MCP-1 gene were constructed. As shown in Fig. 6B and C, the deletion of −70 to +1 resulted in the complete loss of even the basal transcriptional activity of the reporter gene. This is consistent with the report of Ueda *et al.* (32) that the GC box controlling the basal transcriptional activity of MCP-1 gene was located between −64 bp and −59 bp. Fragment −73 to +8, which contains the GC box and TATA box of the MCP-1 gene, was obtained with the primer pair 3+4 (Table 1) and was cloned into the NheI–BglII restriction site of the pGL-3 basic vector. Cloning of fragments −7537 to −2586, −7537 to −2614, −7537 to −2647, and −7537 to −6489 into the Acc 65I (KpnI)-MluI site of the pGL-3 basic vector upstream of the MCP-1 GC box fragment resulted in deletions of fragments −2587 to −74 (D-N-1), −2615 to −74 (D-N-2), −2648 to −74 (D-N-3), and −6488 to −74 (D-N-4) (Fig. 7).

The deletion of −2587 to −74 base pairs (reporter D-N-1; Fig. 7) resulted in a 50% and 55% decrease of the TNF-α– and IL-1β–induced reporter activities. Although the cytokine-induced MCP-1 expression was reduced, DMSO was still able to exhibit significant suppression of the induced reporter activity. Removal of 29 additional nucleotides from −2615 to −2586, which includes the A2 NF-κB binding site (GGGAATTTCC), resulted in essentially complete loss of stimulus-induced reporter activity. Further deletion of the A1 NF-κB binding site (GGGAACTTCC) had no additional suppressive effect on the reporter activities, although it must be acknowledged that the levels were already lowered so dramatically that it would be nearly impossible to observe any further reduction. These data suggest strongly that transcription-factor binding sites in this downstream fragment participated in the maximal expression of the MCP-1 gene.

As shown in Fig. 6, the deletion of −7537 to −6852 resulted in a dramatic decrease of cytokine-induced reporter activities, implying that this fragment plays a role in regulating MCP-1 gene expression. Vector D-N-4 was constructed with deletion

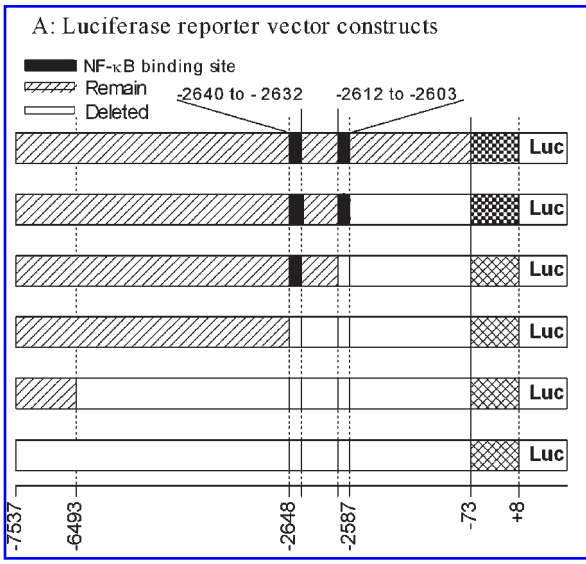

Vector	TNF-α (2 ng/ml)	TNF-α+ DMSO	IL-1β (1 ng/ml)	IL-1β+ DMSO
PGL-3-MCP-1	233±37	104±7	287±14	107±13
D-N-1	118±11	62±3	130±11	67±9
D-N-2	1±1	1±1	4±2	4±1
D-N-3	NHTC	NHTC	NHTC	NHTC
D-N-4	NHTC	NHTC	NHTC	NHTC
D-N-5	NHTC	NHTC	NHTC	NHTC

FIG. 7. Analysis of downstream deletions in the promoter region of MCP-1 gene. The reporter vectors containing downstream deletions were cotransfected, as in Fig. 6. (**A**) The 3′ deletions in the human MCP-1 promoter region linked to the luciferase gene are indicated. The NF-κB binding sites are indicated by *black boxes*. LUC indicates the luciferase gene. *Open boxes*, The deleted fragments. (**B**) The activity of reporter vectors shown from (**A**) is expressed as the ratio of firefly luciferase activity to *Renilla* activity after subtraction of the basal activity. Values are expressed as mean ± SEM, $n = 4$.

of fragment −6488 to −74. D-N-4 induced a minimal amount of reporter activity compared with the other constructs (data not shown) and did not respond to the stimulation with TNF-α or IL-1β. DMSO was without effect because the induced levels were so low. These data indicate that additional elements participated in the maximal expression of the MCP-1 gene, which were dependent on the other elements, especially NF-κB binding sites, but these additional elements were not responsive to TNF-α or IL-1β stimulation.

Effects of mutation or deletion of NF-κB binding sites on reporter activity

The data show that the 5′ or 3′ deletions of the MCP-1 promoter region without altering either the A1 or A2 NF-κB binding sites decreased the magnitude of MCP-1 gene expression, but did not result in complete loss of stimulus-induced transcriptional activity and the inhibition of DMSO. Additional removal of one NF-κB binding site, either in 5′ or 3′ deletion, completely abolished the response to TNF-α and IL-1β. These data strongly imply that the function of the regulatory elements located in either the up- or the downstream position depends on both NF-κB binding sites. To determine the relation between the two NF-κB binding sites, and the dependence of other elements on NF-κB binding sites, mutations at either NF-κB binding sites or deletion of both sites were induced separately on the background of the whole 5′-flanking promoter region of the MCP-1 gene.

As shown in Fig. 8, mutation of the A1 NF-κB binding site (vector N-M-1) resulted in a 76% and 79% decrease of the reporter activity in response to TNF-α and IL-1β, respectively. The mutation at the A2 NF-κB binding site (vector N-M-2) resulted in an 88% and 94% decrease of promoter activity, respectively. These data indicate that the downstream NF-κB binding site was slightly more powerful than the upstream one in controlling TNF-α– and IL-1β–induced MCP-1 gene expression. Although mutation of a single NF-κB binding site decreased MCP-1 gene expression, DMSO was still capable of inhibiting the cytokine induced reporter activity. Deletion of both NF-κB binding sites completely eliminated the reporter response to either TNF-α or IL-1β. Analysis of the mutation and deletion data demonstrated that the regulatory effects of the other elements is dependant on the activity of NF-κB binding sites, including the cooperation between both NF-κB binding sites. Additionally, DMSO inhibited TNF-α– and IL-1β–induced MCP-1 gene expression through affecting the activity of both NF-κB binding sites.

Exogenous ROIs induce MCP-1 gene expression through NF-κB binding sites

As shown earlier, the inhibition of DMSO on TNF-α– and IL-1β–induced MCP-1 gene expression depended on NF-κB binding sites. To identify directly whether ROIs play roles in MCP-1 gene expression through NF-κB binding sites, O_2^- produced by the xanthine-xanthine oxidase (X-XO) system was used to stimulate A549 cells. O_2^- generated by X-XO (1.6 m*M* to 3 mU/ml) for 6 h significantly stimulated A549 cells to produce MCP-1 (259.7 ± 50.1 *vs.* 622.7 ± 105.3 pg/ml, $n = 4$, $p < 0.05$). As shown in Fig. 9, X-XO induced MCP-1 reporter activity in pGL-3-MCP-1, N-M-1, and N-M-2 transfected A549 cells. For each of these reporters, the oxidant-induced activity was nearly completely abolished by DMSO. Mutation of the A1 NF-κB binding site (vector N-M-1) resulted in a 22.4% decrease of the reporter activity in response to X-XO (1.6 m*M* to 3 mU/ml). The mutation at the A2 NF-κB binding site (vector N-M-2) resulted in a 38.3% decrease of promoter activity. These data indicated that the downstream A2 NF-κB binding

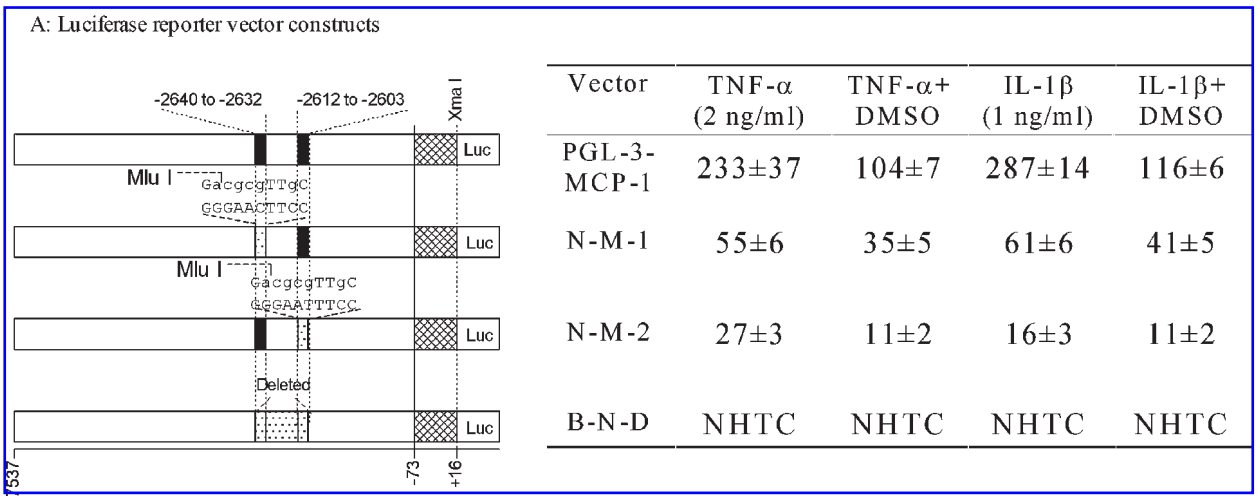

Vector	TNF-α (2 ng/ml)	TNF-α+ DMSO	IL-1β (1 ng/ml)	IL-1β+ DMSO
PGL-3-MCP-1	233±37	104±7	287±14	116±6
N-M-1	55±6	35±5	61±6	41±5
N-M-2	27±3	11±2	16±3	11±2
B-N-D	NHTC	NHTC	NHTC	NHTC

FIG. 8. Analysis of mutations and deletions of NF-κB binding sites in the MCP-1 promoter. (**A**) Vector constructs. NF-κB binding sites are indicated by *black* (not mutated) or *shaded* (mutated) boxes. The lower-case letters indicate the mutated base pairs. N-M-1 and N-M-2 have the NF-κB binding sites mutated, whereas B-N-D has both bindings sites deleted. The MluI restriction site is indicated. (**B**) The activity of reporter vectors shown in (A) is expressed as the ratio of firefly luciferase activity to *Renilla* luciferase activity after subtraction of the basal activity. Values are expressed as mean ± SEM, $n = 4$.

site was slightly more powerful than the upstream one in regulating ROI-induced MCP-1 gene expression, consistent with the data in Fig. 8. Deletion of both NF-κB binding sites (B-N-D) completely eliminated the reporter response to X-XO.

DISCUSSION

In this study, we showed that both TNF-α and IL-1β stimulated MCP-1 mRNA expression and protein production in a similar dose-dependent and kinetic pattern in A549 cells, a human type II alveolar epithelial cell line. We demonstrated that the antioxidant DMSO decreased MCP-1 mRNA expression and protein production in TNF-α– and IL-1β–stimulated A549 cells in dose-dependent manner. DMTU, another antioxidant, also inhibited cytokine-induced MCP-1 protein secretion. By using a reporter vector containing the whole known 5′-flanking region of human MCP-1 and EMSA, we verified that DMSO inhibits cytokine-stimulated MCP-1 production at the transcriptional level through suppressing NF-κB. Moreover, the two proximal NF-κB binding sites(15, 31) are critical for stimulus-induced enhancer activities. Mutation of either of the NF-κB binding sites decreased enhancer activity by TNF-α and IL-1β. Deletion of both sites completely abolished TNF-α– and IL-1β–induced transcriptional activity. To further confirm the importance of these sites, direct stimulation with ROI induced reporter activity, which was significantly reduced by DMSO.

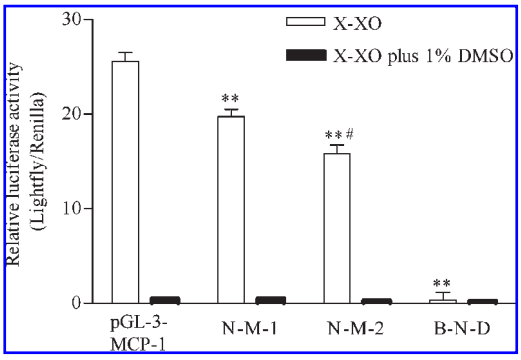

FIG. 9. ROI induction of MCP-1 reporter activity through NF-κB binding sites. After transfection with pGL-3-MCP-1, N-M-1, N-M-2, and B-N-D, as indicated in Fig. 8A, A549 cells were stimulated with X-XO (1.6 m*M* to 3 mU/ml) for 6 h. The induced activity of reporter vectors is expressed as the ratio of firefly luciferase activity to *Renilla* luciferase activity after subtraction of the basal activity. Both NF-κB sites modulate reporter activity. Deletion of both sites completely eliminates the ability of ROIs to induce MCP-1 reporter activity. Values are expressed as mean ± SEM; $n = 3$. $^{**}p < 0.01$ compared with pGL-3-MCP-1. $^{\#}p < 0.05$ compared with N-M-1.

Several recent studies have shown that ROI may act as intracellular second messengers to mediate production of certain chemokines, which are potent chemoattractants for inflammatory cells. In this setting, amplification of tissue damage may also occur through infiltration of inflammatory cells, either acutely or chronically (13). The MCP-1 gene can be induced by numerous stimuli, including cytokines whose functions are partially mediated by ROIs (28). Among the cytokines secreted by infiltrating macrophages, TNF-α and IL-1β are important for the development and regulation of local inflammation and tissue damage (29). DeForge *et al.* (9) and Barrett *et al.* (2) reported that ROIs serve as second messengers to induce IL-8 gene expression in different cells, including human type II alveolar epithelial cells. Fat-storing cells produce MCP-1 in response to oxygen free radical stimulation (37).

Several functional binding sites for transcription factors are present in the 5′-flanking region of the human MCP-1 gene, including NF-κB , Sp 1, AP-1, TRE, and NF-IL-6(11, 21–24, 32). Two closely located NF-κB binding sites, A1 and A2 (31), were

identified in the 5′-flanking region of the human MCP-1 gene (32). Our data showed that the existence of both NF-κB binding sites was important for transcription of the human MCP-1 gene and tightly related to the inhibiting effect of DMSO on MCP-1 gene expression. Other investigators also demonstrated that multiple sites regulate chemokine induction, such as IL-8 (25). The deletion of these two NF-κB binding sites resulted in the complete abolishment of TNF-α– and IL-1β–induced human MCP-1 gene expression, indicating that the regulatory function of other transcription factors for MCP-1 gene expression depends on the activation of these two κB sites. Furthermore, our study supplies information about the relation between the NF-κB binding sites and the other transcription factors. Upstream and downstream deletions of the 5′ flanking region of the MCP-1 gene resulted in a decrease in reporter activity. If only one NF-κB binding site was included in the 5′ or 3′ deletion, the cytokine-induced responses were essentially abolished. This suggests that any other transcription factor binding sites that participate in the stimulus-induced expression of the MCP-1 gene depend on the activation and coexistence of the NF-κB binding sites. The typical example is the deletion of an ~1-kb fragment in the far upstream position of the 5′-flanking region. This deletion resulted in a dramatic decrease of cytokine-induced reporter gene activity through unknown elements located in this fragment, which requires more work to identify. Interestingly, mutation of these sites did not reduce the ability of ROIs to induce promoter activity.

The deletion of 5′ fragments, not including the A1 NF-κB binding site, and 3′ fragments, not including A2 NF-κB binding site, resulted in a partial decrease of cytokine-induced MCP-1 promoter activities, but the inhibiting potential of DMSO was not altered. The 5′ or 3′ deletion that included only one NF-κB binding site resulted in near-complete abolishment of cytokine-induced MCP-1 promoter activity, indicating that the inhibition of DMSO directly related to the two κB sites and that the elements located in the upstream or downstream fragment of both κB sites are not involved in the inhibition of DMSO. The electromobility shift assay data confirmed that DMSO inhibited proinflammatory cytokine-induced NF-κB activation. More-direct evidence showed that exogenous ROIs induce MCP-1 gene expression in A549 cells through the two NF-κB binding sites, which was inhibited by DMSO. As a free radical scavenger and antioxidant, DMSO has been found to inhibit the activation of the NF-àB in a number of cell lines. Kelly *et al.* (14) reported that DMSO decreased the level of LPS-induced NF-κB activation in the J774 macrophage-like cell line. DMSO also inhibited X/XO induced increases in NF-κB and MCP-1 production from U937 cells (17). These observations were extended to the *in vivo* setting, where therapeutic treatment with DMSO inhibited sepsis-induced activation of NF-κB and AP-1, resulting in the suppression of ICAM-1 gene expression in the livers of septic rats (4, 5). In galactosamine-sensitized C3Heb/FeJ mice, DMSO effectively inhibited endotoxin- and TNF-α–induced hepatic NF-àB activation (10). These previous reports and our present data demonstrate the importance of ROIs in the regulation of MCP-1 production, and by extension, regulation of inflammation.

Besides inhibiting the direct damage of ROI produced by infiltrating leukocytes, antioxidants could also inhibit ROI-mediated chemokine production from inflammatory cells. Decreased chemokine production should result in decreased inflammatory cell recruitment. We demonstrated here that the human alveolar type II cell line, A549, was able to produce the CC chemokine MCP-1 in response to proinflammatory cytokines. DMSO significantly inhibited this chemokine synthesis. The data imply that one more mechanism supports antioxidant treatment in lung injury. Antioxidants inhibited the ROI-mediated chemokine production from the nonimmune cells, the resident cells, at the local inflammatory site. This will consequently result in decreased leukocyte infiltration and ROI production.

With the poly-riboprobe set, we did not detect mRNA expression for chemokines other than MCP-1 and IL-8. These agree with those of Lakshminarayanan *et al.* (16), who also did not detect mRNA expression of Ltn, IP-10, MIP-1α, MIP-1β, and I-309 in TNF-α–treated A549 cells by using the same poly-riboprobe set.

Our study suggests that decreasing intracellular ROIs induced by proinflammatory cytokine stimulation has the potential to decrease inflammatory cell infiltration by lowering the production of chemokines. The mechanism of this attenuated chemokine production occurs *via* inhibition of the transcriptional regulatory factor NF-κB, which binds to specific promoter elements in the MCP-1 gene. These data imply that a portion of the beneficial effects of antioxidants may be through selective reduction of the synthesis of chemokines.

ACKNOWLEDGMENTS

We acknowledge the editorial assistance of Jill Granger in preparing the manuscript. This work was partially supported by the NIH grant GM 50401.

ABBREVIATIONS

DMEM, Dulbecco's modified Eagle's medium; EMSA, electrophoretic mobility shift assay; LPS, lipopolysaccharide; MCP-1, monocyte chemoattractant protein-1; ROIs, reactive oxygen intermediates; RPA, ribonuclease protection assay; TMB, 3,3′,5,5′-tetramethylbenzidine; X/XO, xanthine plus xanthine oxidase.

REFERENCES

1. Baggiolini M, Dewald B, and Moser B. Interleukin-8 and related chemotactic cytokines: CXC and CC chemokines. *Adv Immunol* 55: 97–179, 1994.
2. Barrett EG, Johnston C, Oberdorster G, and Finkelstein JN. Antioxidant treatment attenuates cytokine and chemokine levels in murine macrophages following silica exposure. *Toxicol Appl Pharmacol* 158: 211–220, 1999.
3. Call DR, Nemzek JA, Ebong SJ, Bolgos GL, Newcomb DE, and Remick DG. Ratio of local to systemic chemokine concentrations regulates neutrophil recruitment. *Am J Pathol* 158: 715–721, 2001.
4. Chang CK, Albarillo MV, and Schumer W. Therapeutic effect of dimethyl sulfoxide on ICAM-1 gene expression and activation of NF-kappaB and AP-1 in septic rats. *J Surg Res* 95: 181–187, 2001.
5. Chang CK, Llanes S, and Schumer W. Inhibitory effect of dimethyl sulfoxide on nuclear factor-kappa B activation and intercellular adhesion molecule 1 gene expression in septic rats. *J Surg Res* 82: 294–299, 1999.

6. Chen XL, Zhang Q, Zhao R, and Medford RM. Superoxide, H2O2, and iron are required for TNF-alpha-induced MCP-1 gene expression in endothelial cells: role of Rac1 and NADPH oxidase. *Am J Physiol Heart Circ Physiol* 286: H1001–H1007, 2004.
7. Chomczynski P and Sacchi N. Single-step method of RNA isolation by acid guanidinium thiocyanate-phenol-chloroform extraction. *Analyt Biochem* 162: 156–159, 1987.
8. DeForge LE, Fantone JC, Kenney JS, and Remick DG. Oxygen radical scavengers selectively inhibit interleukin 8 production in human whole blood. *J Clin Invest* 90: 2123–2129, 1992.
9. DeForge LE, Preston AM, Takeuchi E, Kenney J, Boxer LA, and Remick DG. Regulation of interleukin 8 gene expression by oxidant stress. *J Biol Chem* 268: 25568–25576, 1993.
10. Essani NA, Fisher MA, and Jaeschke H. Inhibition of NF-kappa B activation by dimethyl sulfoxide correlates with suppression of TNF-alpha formation, reduced ICAM-1 gene transcription, and protection against endotoxin-induced liver injury. *Shock* 7: 90–96, 1997.
11. Finzer P, Soto U, Delius H, Patzelt A, Coy JF, Poustka A, zur Hausen H, and Rosl F. Differential transcriptional regulation of the monocyte-chemoattractant protein-1 (MCP-1) gene in tumorigenic and non-tumorigenic HPV 18 positive cells: the role of the chromatin structure and AP-1 composition. *Oncogene* 19: 3235–3244, 2000.
12. Geng Z, Rong Y, and Lau BH. S-allyl cysteine inhibits activation of nuclear factor kappa B in human T cells. *Free Radic Biol Med* 23: 345–350, 1997.
13. Holzer K, Richter A, Henrich D, Wilhelm K, and Encke A. Oxygen radical generation by emigrated, intra-abdominal, and circulating PMNLs during human secondary peritonitis. *Shock* 15: 90–94, 2001.
14. Kelly KA, Hill MR, Youkhana K, Wanker F, and Gimble JM. Dimethyl sulfoxide modulates NF-kappa B and cytokine activation in lipopolysaccharide-treated murine macrophages. *Infect Immun* 62: 3122–3128, 1994.
15. Kutlu B, Darville MI, Cardozo AK, and Eizirik DL. Molecular regulation of monocyte chemoattractant protein-1 expression in pancreatic beta-cells. *Diabetes* 52: 348–355, 2003.
16. Lakshminarayanan V, Beno DW, Costa RH, and Roebuck KA. Differential regulation of interleukin-8 and intercellular adhesion molecule-1 by H2O2 and tumor necrosis factor-alpha in endothelial and epithelial cells. *J Biol Chem* 272: 32910–32918, 1997.
17. Lee JS, Kahlon SS, Culbreth R, and Cooper AD Jr. Modulation of monocyte chemokine production and nuclear factor kappa B activity by oxidants. *J Interferon Cytokine Res* 19: 761–767, 1999.
18. Liu Y, Tergaonkar V, Krishna S, and Androphy EJ. Human papillomavirus type 16 E6-enhanced susceptibility of L929 cells to tumor necrosis factor alpha correlates with increased accumulation of reactive oxygen species. *J Biol Chem* 274: 24819–24827, 1999.
19. Ndengele MM, Muscoli C, Wang ZQ, Doyle TM, Matuschak GM, and Salvemini D. Superoxide potentiates NF-kappaB activation and modulates endotoxin-induced cytokine production in alveolar macrophages. *Shock* 23: 186–193, 2005.
20. Nemzek JA, Siddiqui J, and Remick DG. Development and optimization of cytokine ELISAs using commercial antibody pairs. *J Immunol Methods* 255: 149–157., 2001.
21. Ping D, Boekhoudt G, and Boss JM. *trans*-Retinoic acid blocks platelet-derived growth factor-BB-induced expression of the murine monocyte chemoattractant-1 gene by blocking the assembly of a promoter proximal Sp1 binding site. *J Biol Chem* 274: 31909–31916, 1999.
22. Ping D, Boekhoudt G, Zhang F, Morris A, Philipsen S, Warren ST, and Boss JM. Sp1 binding is critical for promoter assembly and activation of the MCP-1 gene by tumor necrosis factor. *J Biol Chem* 275: 1708-1714, 2000.
23. Ping D, Boekhoudt GH, Rogers EM, and Boss JM. Nuclear factor-kappa B p65 mediates the assembly and activation of the TNF-responsive element of the murine monocyte chemoattractant-1 gene. *J Immunol* 162: 727–734, 1999.
24. Ping D, Jones PL, and Boss JM. TNF regulates the in vivo occupancy of both distal and proximal regulatory regions of the MCP-1/JE gene. *Immunity* 4: 455–469, 1996.
25. Rodgers HC, Pang L, Holland E, Corbett L, Range S, and Knox AJ. Bradykinin increases IL-8 generation in airway epithelial cells via COX-2-derived prostanoids. *Am J Physiol Lung Cell Mol Physiol* 283: L612–618., 2002.
26. Rosseau S, Hammerl P, Maus U, Walmrath HD, Schutte H, Grimminger F, Seeger W, and Lohmeyer J. Phenotypic characterization of alveolar monocyte recruitment in acute respiratory distress syndrome. *Am J Physiol Lung Cell Mol Physiol* 279: L25–L35, 2000.
27. Saetre T, Kahler H, Foster SJ, and Lyberg T. Aminoethyl-isothiourea inhibits leukocyte production of reactive oxygen species and proinflammatory cytokines induced by streptococcal cell wall components in human whole blood. *Shock* 15: 455–460, 2001.
28. Satriano JA, Schuldiner M, Hora K, Xing Y, Shan Z, and Schlondorff D. Oxygen radicals as second messengers for expression of the monocyte chemoattractant protein, JE/MCP-1, and the monocyte colony-stimulating factor, CSF-1, in response to tumor necrosis factor alpha and immunoglobulin G: evidence for involvement of reduced nicotinamide adenine dinucleotide phosphate (NADPH)-dependent oxidase. *J Clin Invest* 92: 1564–1571, 1993.
29. Simons RK, Junger WG, Loomis WH, and Hoyt DB. Acute lung injury in endotoxemic rats is associated with sustained circulating IL-6 levels and intrapulmonary CINC activity and neutrophil recruitment: role of circulating TNF-alpha and IL-beta? *Shock* 6: 39–45, 1996.
30. Tanaka C, Kamata H, Takeshita H, Yagisawa H, and Hirata H. Redox regulation of lipopolysaccharide (LPS)-induced interleukin-8 (IL-8) gene expression mediated by NF kappa B and AP-1 in human astrocytoma U373 cells. *Biochem Biophys Res Commun* 232: 568–573, 1997.
31. Ueda A, Ishigatsubo Y, Okubo T, and Yoshimura T. Transcriptional regulation of the human monocyte chemoattractant protein-1 gene: cooperation of two NF-kappaB sites and NF-kappaB/Rel subunit specificity. *J Biol Chem* 272: 31092–31099, 1997.
32. Ueda A, Okuda K, Ohno S, Shirai A, Igarashi T, Matsunaga K, Fukushima J, Kawamoto S, Ishigatsubo Y, and Okubo T. NF-kappa B and Sp1 regulate transcription of the human monocyte chemoattractant protein-1 gene. *J Immunol* 153: 2052–2063, 1994.
33. Umekawa T, Iguchi M, Uemura H, and Khan SR. Oxalate ions and calcium oxalate crystal-induced up-regulation of osteopontin and monocyte chemoattractant protein-1 in renal fibroblasts. *BJU Int* 98: 656–660, 2006.
34. Valente AJ, Graves DT, Vialle-Valentin CE, Delgado R, and Schwartz CJ. Purification of a monocyte chemotactic factor secreted by nonhuman primate vascular cells in culture. *Biochemistry* 27: 4162–4168, 1988.
35. Witowski J, Thiel A, Dechend R, Dunkel K, Fouquet N, Bender TO, Langrehr JM, Gahl GM, Frei U, and Jorres A. Synthesis of C-X-C and C-C chemokines by human peritoneal fibroblasts: induction by macrophage-derived cytokines. *Am J Pathol* 158: 1441–1450, 2001.
36. Xing L and Remick DG. Mechanisms of dimethyl sulfoxide augmentation of IL-1 beta production. *J Immunol* 174: 6195–6202, 2005.
37. Xu Y, Rojkind M, and Czaja MJ. Regulation of monocyte chemoattractant protein 1 by cytokines and oxygen free radicals in rat hepatic fat-storing cells. *Gastroenterology* 110: 1870–1877, 1996.

Address reprint requests to:
Daniel Remick
Department of Pathology
University of Michigan Medical School
M2210 Medical Science Building 1
1301 Catherine Road
Ann Arbor, MI 48109

E-mail: remickd@bu.edu

Date of first submission to ARS Central, September 13, 2007; date of acceptance, September 13, 2007.

This article has been cited by:

1. Savita Khanna , Han-A Park , Chandan K. Sen , Trimurtulu Golakoti , Krishanu Sengupta , Somepalli Venkateswarlu , Sashwati Roy . 2009. Neuroprotective and Antiinflammatory Properties of a Novel Demethylated CurcuminoidNeuroprotective and Antiinflammatory Properties of a Novel Demethylated Curcuminoid. *Antioxidants & Redox Signaling* **11**:3, 449-468. [Abstract] [PDF] [PDF Plus]
2. Sushil K. Jain , Justin Rains , Jennifer Croad , Bryon Larson , Kimberly Jones . 2009. Curcumin Supplementation Lowers TNF-α, IL-6, IL-8, and MCP-1 Secretion in High Glucose-Treated Cultured Monocytes and Blood Levels of TNF-α, IL-6, MCP-1, Glucose, and Glycosylated Hemoglobin in Diabetic RatsCurcumin Supplementation Lowers TNF-α, IL-6, IL-8, and MCP-1 Secretion in High Glucose-Treated Cultured Monocytes and Blood Levels of TNF-α, IL-6, MCP-1, Glucose, and Glycosylated Hemoglobin in Diabetic Rats. *Antioxidants & Redox Signaling* **11**:2, 241-250. [Abstract] [PDF] [PDF Plus]
3. Shyam Biswal , Daniel G. Remick . 2007. Sepsis: Redox Mechanisms and Therapeutic OpportunitiesSepsis: Redox Mechanisms and Therapeutic Opportunities. *Antioxidants & Redox Signaling* **9**:11, 1959-1962. [Citation] [PDF] [PDF Plus]